Advanced Materials Research Vol. 325 (2011) pp 35-41
Online available since 2011/Aug/22 at www.scientific.net

doi:10.4028/www.scientific.net/AMR.325.35

Heat Transfer in Grinding-Hardening of a Cylindrical Component

Thai Nguyen[1, a], Liang Chi Zhang[1, b] and Dale Sun[2, c]

[1]School of Mechanical and Manufacturing Engineering
The University of New South Wales, NSW 2052, Australia

[2]Equipment Research Department, Research Institute,
Baoshan Iron & Steel Co., Ltd., Fujin Road, Baoshan, Shanghai 201900, PR China

[a]thai.nguyen@unsw.edu.au, [b]liangchi.zhang@unsw.edu.au, [c]sundl@baosteel.com

Keywords: Grinding-hardening; Cylindrical grinding; Temperature field; Moving heat source

Abstract. A three-dimensional finite element heat transfer model incorporating a moving heat source was developed to investigate the heat transfer mechanism in grinding-hardening of a cylindrical component. The model was applied to analyze the grinding-hardening of quenchable steel 1045 by two grinding methods, traverse and plunge grinding. It was found that the heat generated can promote the martensitic phase transformation in the ground workpiece. As a result, a hardened layer with a uniform thickness can be produced by traverse grinding. However, the layer thickness generated by plunge grinding varies circumferentially. The results are in good agreement with the experimental observations.

Introduction

Grinding-hardening is a technique that uses the heat generated in grinding to create a hardened surface layer by promoting the phase transformation in a steel component. The layer hardened in this way has a remarkable improvement in resistance of wear and fatigue [1 - 2].

The kinetics of phase transformations in grinding-hardening, unlike that in a conventional heat treatment process, is complex and depends greatly on the temperature and time during grinding[3]. The grinding heat source is generated within a small wheel-workpiece interaction zone and moves on the grinding surface during the process. In the grinding of a curved surface, the heat source follows two motions, one is the rotation about the workpiece axis and the other is associated with the feed of the grinding wheel. While the heat source is moving, the material in its vicinity experiences convective cooling. The heat transfer analysis of grinding to date, however, is limited to 2D surface grinding, which is very different from the case with cylindrical grinding [4].

This study aims to understand the three-dimensional, transient heat transfer process during grinding-hardening of a cylinder. The finite element method will be used. Two typical processes, plunge and traverse grinding, will be investigated.

Modeling

The calculation of the temperature field was based on a 3D unsteady-state heat conduction equation, applying on a cylinder [5] (Fig. 1):

$$\frac{1}{r}\frac{\partial}{\partial r}\left(kr\frac{\partial T}{\partial r}\right)+\frac{1}{r^2}\frac{\partial}{\partial \theta}\left(k\frac{\partial T}{\partial \theta}\right)+\frac{\partial}{\partial z}\left(k\frac{\partial T}{\partial z}\right)+\dot{q}_g=\rho C_p\frac{\partial T}{\partial t} \quad (1)$$

where $\dot{q}_g$ is the heat rate per unit volume during phase transformation[4, 6], k, ρ and C_p are the thermal conductivity, density and specific heat of workpiece material, respectively, and are temperature dependent. The commercially available software, ANSYS, will be used for the solution of the equation, incorporating temperature and time dependence of these parameters. The initial and boundary conditions for the solution of the equation are as follows:

Initial conditions

$$T(r,z,t)\big|_{t=0} = T_\infty = 22^o C, 0 \le r \le R_w \text{ and } 0 \le z \le L \tag{2}$$

where T_∞ is the ambient temperature, R_w and L are the initial radius and length of the workpiece.

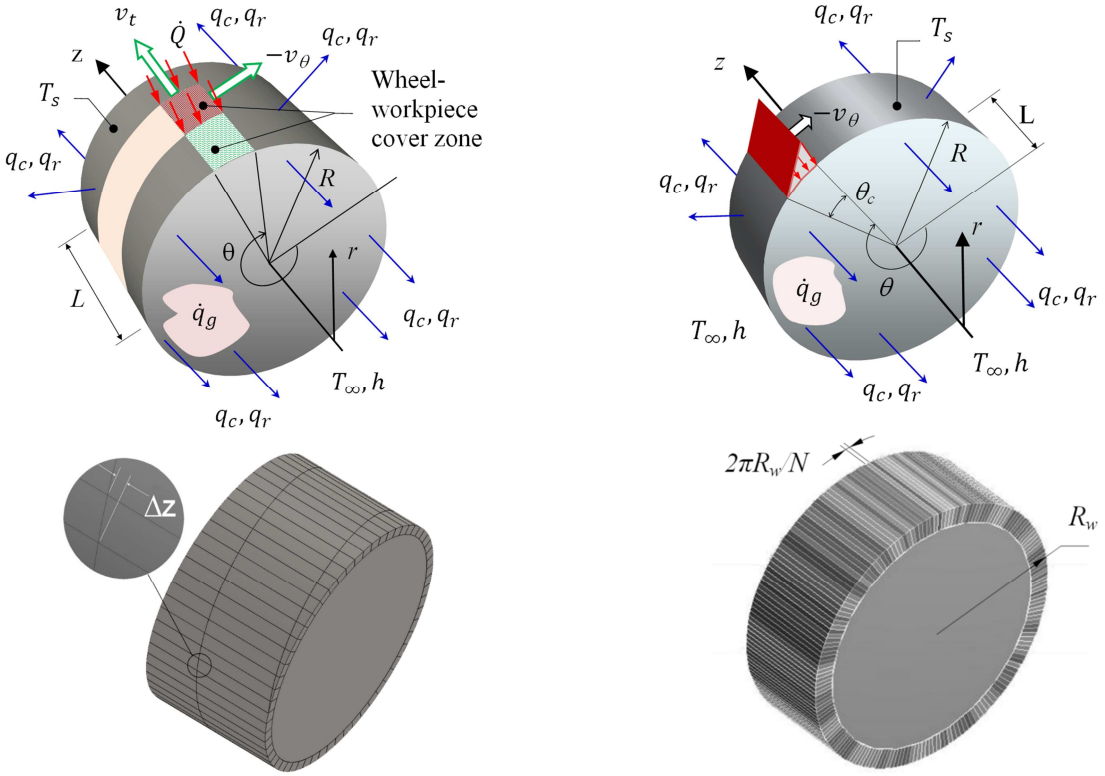

(a) Traverse grinding (b) Plunge grinding

Fig. 1. Thermal conduction and mesh-generation

Boundary condition for heating by the moving heat source. The grinding heat can be regarded as a heat source sliding on the workpiece surface with the same velocity as that of the workpiece but in opposite direction, when the workpiece is regarded as a static body.

- In *traverse grinding*, the workpiece rotates about its axis with angular velocity $\omega$and is fed with the grinding wheel in the z-direction with a feed rate v_z. The workpiece was meshed with a spiral configuration associated with the motion profile as shown in Fig. 1(a). The peripheral surface where the sliding heat was applied was divided in the circumferential direction by N_c uniform divisions and in the longitudinal direction with a step increment of $\Delta z = 2v_z\pi/\omega N_c$.

The heat flow $\dot{Q}(t)$ applied on the n^{th} element can be derived as

$$\dot{Q}(t) = \begin{cases} \eta u_g \dot{V}_n & (n\text{-}1)\Delta t \le t \le n\Delta t \\ 0 & t < (n-1)\Delta t \cup t > n\Delta t \end{cases} \tag{3}$$

where($\Delta t = 2\pi/N_c\omega$) is the time required for the heat source moving in a step increment Δz, η is the fraction of total energy conducted as heat into the workpiece (heat partition ratio), determined according to Ref. [4]. $u_g\,(J/mm^3)$ is the specific grinding energy which can be determined based on the correlated data[6]:

$$u_g = 61.64\dot{V}''^{-0.176} \tag{4}$$

in which a is the depth of cut, and $\dot{V}''\,(mm^3/mm.s)$ is the specific material removal rate per unit wheel width:

$$\dot{V}'' = a\omega \frac{R_w(2R_w - a)}{2(R_w - a)} \tag{5}$$

The volumetric material removal rate associated with the n^{th} element ($\dot{V}_n$) is determined by

$$\dot{V}_n = \frac{\pi}{N_c \Delta t}[R_w^2 - (R_w - a)^2]\bar{l}_n \tag{6}$$

It is necessary to highlight that during the first and the last revolutions of the workpiece in traverse grinding, the depth of cut is a constant but the grinding wheel does not contact with the workpiece entirely by its width. As such, the average ground width of the n^{th} element ($\bar{l}_n$) varies continuously. However, in the zone associated with ($L/\Delta z > n > N_c$), the wheel surface overlaps with the surface ground from a previous revolution of workpiece. Although the total longitudinal feed $z(t)$ increases during the operation, the average ground width is a constant. Therefore,

$$\begin{cases} \bar{l}_n = (n - 0.5)\Delta z, & n \le N_c \ (first\ revolution) \\ \bar{l}_n = \left(\dfrac{L}{\Delta z} + N_c + 0.5 - n\right)\Delta z & n \ge L/N_c \ (last\ revolution) \\ \bar{l}_n = N_c \Delta z, & L/\Delta z > n > N_c \end{cases} \tag{7}$$

• In *plunge grinding*, the workpiece was meshed by dividing its circumference surface with N equal elements, as shown in Fig. 1(b). The heat flux variation with respect to the time applied on the n^{th} element can be derived as:

$$q(n,t) = \begin{cases} q_p\left(1 - \dfrac{t - (n-1)t_0}{T}\right), & (n-1)t_0 \le t \le (n-1)t_0 + T_0 \\ 0, & t < (n\text{-}1)t_0 \cup t > n-1)t_0 + T_0 \end{cases} \tag{8}$$

where $t_0 = 2\pi/(N\omega)$ and $T_0 = l_c/(R_w\omega)$ are the time intervals that the heat source spends to move over the distances of a unit length and of the contact length ($l_c = \sqrt{\dfrac{2aR_s}{1 + R_s/(R_w - a)}}$ [7]), respectively, in which R_s is the grinding wheel radius. With the approximation of a triangular heat flux profile [8], the peak heat flux, q_p can be determined as

$$q_p = 2\eta \frac{u_g \dot{V}''}{l_c} \tag{9}$$

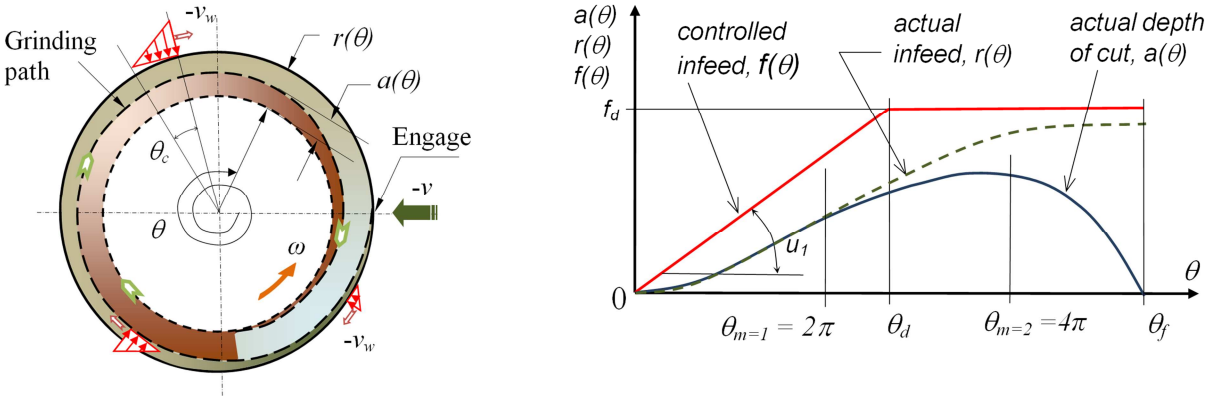

Fig. 2. Variation of depth of cut in plunge cylindrical grinding.

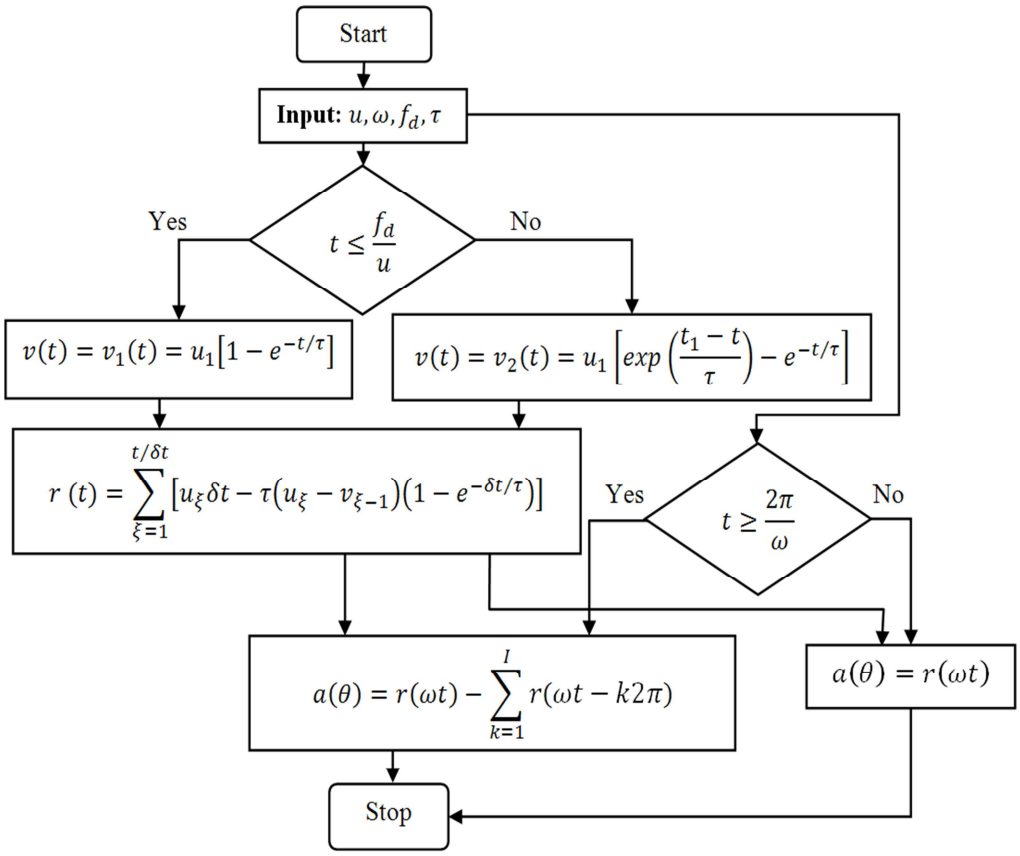

Fig. 3. Flow chart for calculating the depth of cut in plunge cylindrical grinding.

Different from the traverse grinding described previously, in the present plunge grinding the ground width does not change, but the depth of cut (a) varies in the process due to the feeding in the r direction. Because of the deflection of the grinding system, the actual infeed rate (v) corresponding to the reduction in radial dimension of the workpiece is less than the controlled infeed rate (u) of the machine [9], as shown in Fig. 2. The actual depth of cut, $a(\theta)$, with respect to the angular position θ after k cycles on the workpiece can be determined by following the flow chart in Fig. 3, where f_d is the designed total infeed and τ denotes the characteristic time constant of a dynamic grinding system varying from 0.5 to 1.0 s [9].

Boundary condition for cooling. The heat dissipated as cooling mainly contributed to convection, *i.e.*,

$$-k\frac{\partial T}{\partial \vec{n}} = h(T_s - T_\infty) \tag{10}$$

where $\vec{n}$ is the unit vector normal to the surface of a boundary, and T_s is the surface temperature.

The convective heat transfer (coefficient h) occurs on both the side surfaces of the cylinder with their normals of $\vec{n}_z$ and $-\vec{n}_z$, respectively, and on the cylindrical surface of the workpiece. The values of the convective heat transfer coefficient h are determined as

$$h\big|_{z=0} = h\big|_{z=L} = h_a \tag{11}$$

$$h(\theta, z)\big|_{r=R_w} = \begin{cases} 0, & (\theta, z) \in (\theta, z)_{ws} \quad \textit{(within the wheel - workpiece contact zone)} \\ h_a, & (\theta, z) \notin (\theta, z)_{ws} \quad \textit{(outside the wheel - workpiece contact zone)} \end{cases} \tag{12}$$

where h_a is the heat transfer coefficient due to air flow, estimated following the Hilbert's empirical relation for a circular cylinder with radius R_w subjected to a cross flow of air [5]:

$$Nu = \frac{2h_a R_w}{k_a} = CRe^m Pr^{1/3}$$

$$\begin{cases} 4\times10^3 < Re = \dfrac{2v_s R_w}{\upsilon} < 4\times10^4 : C = 0.193, m = 0.618 \\ 4\times10^3 \le Re < 4\times10^6 : C = 0.027, m = 0.805 \end{cases} \quad (13)$$

in which k_a and υ are the thermal conductivity and viscosity of air, respectively. *Nu*, *Pr* and *Re* are the Nusselt, Prandtl and Reynolds numbers, respectively.

Results and discussion

Experiments were conducted on 1045 steel sample with the diameter of 40 mm using a Jones-Shipman cylindrical grinder. The grinding conditions used were: alumina grinding wheel 57A60LV with diameter (mm)/width (mm) = 290/20 and speed of 1,750 rpm; work speed v_w = 40 rpm. For traverse grinding, the specimen length L(mm) = 21, feed rate v_z(mm/s) = 8.4, and depth of cut a(mm) = 0.127. For plunge grinding, L (mm) = 15, controlled infeed rate u_1 (mm/rev) = 0.127 with the designed total infeed f_d (μm) = 200.

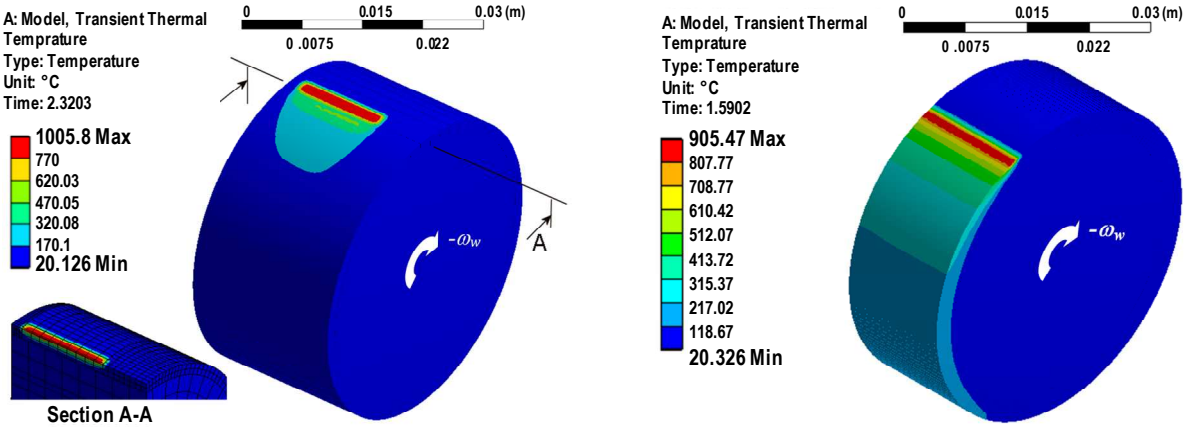

(a) traverse grinding (b) plunge grinding

Fig. 4. Temperature field generated on the workpieces.

Figs. 4(a) and 4(b) show the simulation results of temperature fields developed in the workpieces by the traverse and plunge grinding processes. When the heat source moved along the workpiece surface, the highest temperature rise was within the wheel-workpiece contact zone. In the traverse grinding, the field was in a spiral shape associated with the trajectory of the heat source sweeping on the peripheral workpiece surface.

Fig. 5 shows the temperature history in the ground surfaces. The workpieces experienced frequent heating and cooling cycles. The development of a hardened layer in steel is a result of phase transformations, where the steel is heated to a temperature above the Ac3, held for a sufficient dwell time for the transformation of pearlite to austenite to occur, and then rapidly quenched to the Ms temperature [3]. For instance, by a rapid heating with the rate of 10^4 K/s, the dwell time is only about 10 ms[10] and the quenching rate from the Ac3 of 770 °C required for the martensitic transformation in steel 1045 is less than 200 K/s [11]. In traverse grinding, except the two ends of the workpiece where the wheel was engaged at (θ_1, z = 0.5 mm) and freedat (θ_3, z = 20.5 mm), the conditions for the martensitic formation were satisfied with the peak temperature rose at about 1,050°C. Material at the two unsteady positions cannot be hardened but experiences an annealing. In contrast, temperature profiles obtained from different circumference positions of the material ground by the plunge method varied. The peak temperature that can activate the phase transformation was a result of the heat accumulation from the consequent rotations of the workpiece. After the transformation, material experienced a tempering due to the reheating at temperatures lower than Ac3.

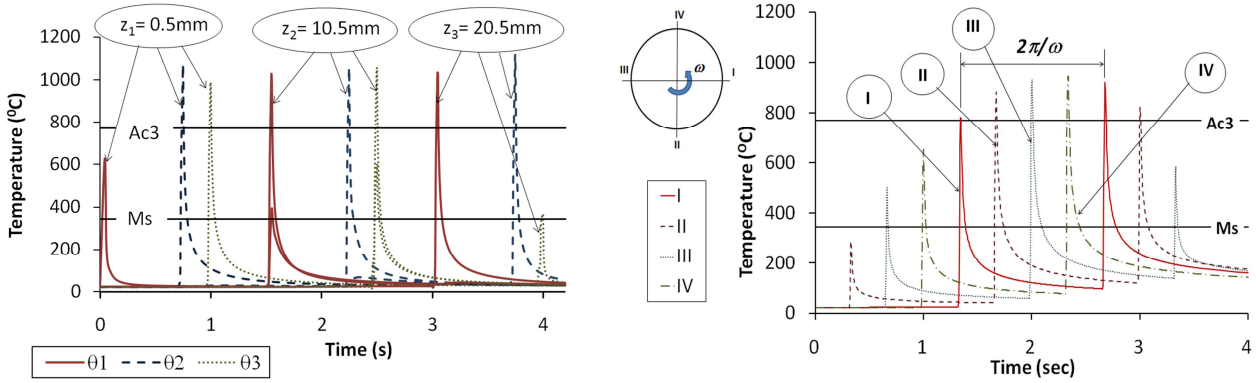

(a) traverse grinding, (θ_1(rad) = π/60, θ_2= π and θ_3 = (1 + 19/60)π).

(b) plunge grinding, wheel-workpiece engaging at position I

Fig. 5. Temperature history in workpiece surfaces.

By probing the peak temperature developed at the Ac3 at subsurface distance of the workpiece, the thickness of the hardened layer can be estimated. Figs. 6 and 7 show the hardened layer thickness obtained by grinding-hardening under traverse and plunge grinding processes, respectively. The average hardness of the hardened layers was 707 HV(500 g load), much higher than that from an ordinary quenching (560 HV) [2](The original hardness of steel 1045 is about 250 HV). In traverse grinding, at position θ_1, up to the distance of z= 140 μm, the temperature rise was not sufficient to make the phase transformation happen. There is an unsteady region (z_u) where the hardened layer thickness varies prior to reaching a constant value (δ). The prediction, Fig. 6(a), shows that z_u = 600 μm and δ = 70 μm, which agree well with the experimental results of z_u = 400 μm δ = 65 μm (Fig. 6(b)). In plunge grinding, on the other hand, the hardened layer is uniform in the (r, z) plane (Fig. 7(a)). However, the layer thickness varies circumferentially, from 37 μm to 116 μm (89.2 μm in average), as shown in Fig. 7(b).

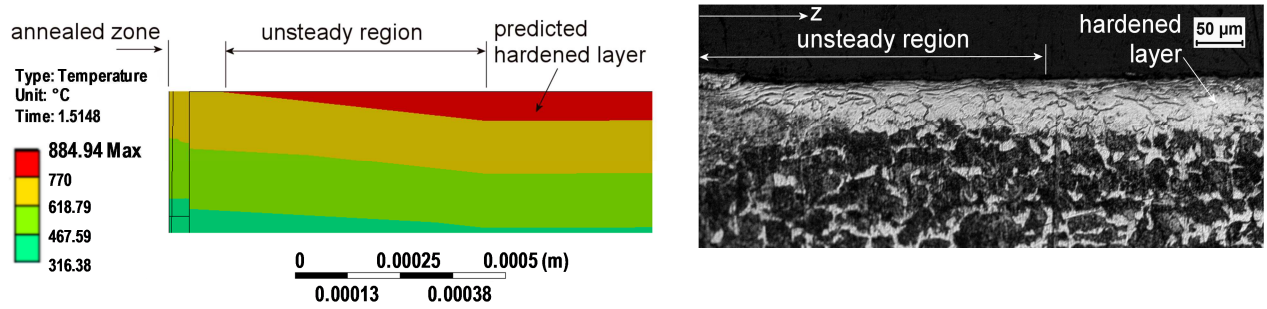

(a) Prediction

(b) Experiment

Fig. 6. Hardened layer thickness along z-direction (at θ_1 (rad) = π/60) generated by traverse grinding.

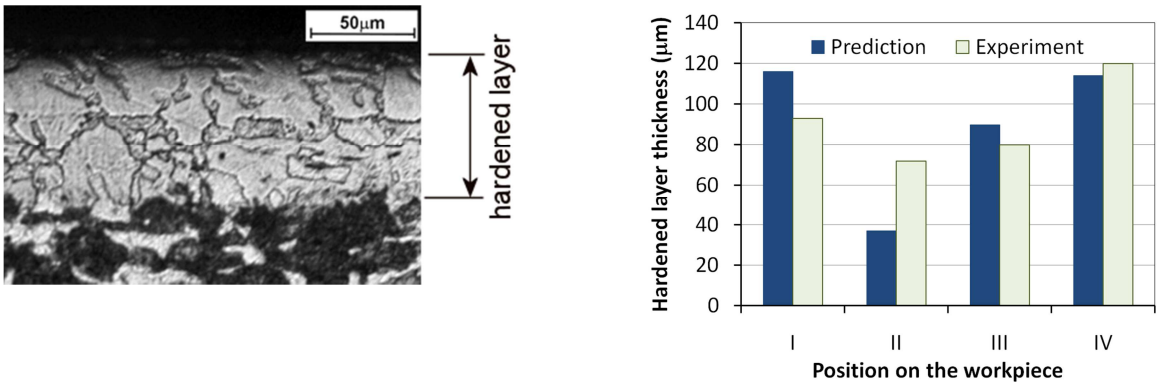

(a) Hardened layer at position III in the (r, z) plane

(b) Variation of the hardened layer thickness in the (r, θ) plane

Fig. 7. Hardened layer thickness generated by plunge grinding.

Conclusion

The above study concludes that the heat generated in traverse and plunge grinding processes can introduce martensitic phase transformation in the ground workpiece. The hardened layer by traverse grinding was uniform, except at the engagement and cease positions between the wheel and the workpiece. The circumferential distribution of the hardened layer in a workpiece by plunge grinding varies.

Acknowledgement

This project was financially supported by the Australian Research Council and Baoshan Iron & Steel Co. Ltd China.

References

[1] I. Zarudi and L.C. Zhang, J. Mater. Sci. 37(18) (2002), p. 3935-3943

[2] T. Nguyen, I. Zarudi, and L.C. Zhang, Int. J. Mach. Tls & Manuf. 47(1) (2007), p. 97-106

[3] H. Bhadeshia: *Bainite in steels - transformations, microstructure and properties* (The University Press, Cambridge 2001)

[4] T. Nguyen and L.C. Zhang, Int. J. Mach. Tls & Manuf. 50(10) (2010), p. 901-910

[5] F.P. Incropera and D.P. Dewitt: *Fundamentals of heat and mass transfer* (J. Wiley & Sons, 1990)

[6] T. Nguyen and L.C. Zhang, Int. J. Mach. Tls & Manuf. 51(4) (2011), p. 309-319

[7] M.C. Shaw: *Principles of abrasive processing* (Oxford University Press 1996)

[8] I. Zarudi and L.C. Zhang, Int. J. Mach. Tls & Manuf. 42(8) (2002), p. 905-913

[9] S. Malkin and C. Guo: *Grinding technology - Theory and applications of machining with abrasives* (Industrial Press 2008)

[10] E. Ohmura, K. Inoue, and K. Haruta, JSME Int. J., Series 1: Solid Mechanics, Strength of Materials 32(1) (1989), p. 45-53

[11] G.E. Totten, M.A.H. Howes, and T. Inoue: *Handbook of residual stress and deformation of steel* (ASM International 2002)

Advances in Abrasive Technology XIV
doi:10.4028/www.scientific.net/AMR.325

Heat Transfer in Grinding-Hardening of a Cylindrical Component
doi:10.4028/www.scientific.net/AMR.325.35